

# Gas entrainment at a propagating slug front

**Problem presented by**

Ruben Schulkes

*Hydro Oil & Energy*

**Problem statement**

When oil is produced, the reservoir pressure decreases and the oil flow rate decreases in proportion to the decreasing pressure difference between the reservoir and the processing facility. At low oil flow rates, a well becomes unstable and this leads to reduced production and processing problems. The formation of slug flow in pipelines is a manifestation of such instability. The front of a slug may be regarded as a propagating, continuously breaking wave, which continuously entrains gas. The Study Group was asked to explore alternative or new ways to treat the gas entrainment problem, to improve understanding of physical processes governing entrainment and to suggest models for the various phenomena. The Study Group obtained mathematical models of slug propagation in horizontal and inclined pipelines, examined possible models of gas entrainment, and outlined an approach to modelling the onset of slug flow. This report summarises that work, and it suggests directions for further investigation.

## **Study Group contributors**

Robert Bauer (University of Oxford)  
Steven Baxter (University of Nottingham)  
Christopher Bell (University of Oxford)  
Richard Booth (University of Oxford)  
John Byatt-Smith (University of Edinburgh)  
Rebecca Carter (University of Oxford)  
Paul Dellar (Imperial College London)  
John Fozard (University of Nottingham)  
Pragnesh Gajjar (University of Nottingham)  
John Garratt (University of Nottingham)  
Andriy Hold (University of Eindhoven)  
Sarah McBurnie (University of Oxford)  
Andrejs Novikovs (University of Oxford)  
John Ockendon (University of Oxford)  
Dharesh Patel (University of Baroda)  
Peter Stewart (University of Nottingham)  
Burt Tilley (Franklin W. Olin College of Engineering)  
Jean-Marc Vanden-Broeck (University of East Anglia)

## **Report prepared by**

Melvin Brown (Smith Institute)  
Paul Dellar (Imperial College London)

# 1 Introduction

## 1.1 Background and motivation

The growing world deficit between oil discovery and consumption makes optimising production from existing fields increasingly important. When oil is produced, the reservoir pressure decreases and the oil flow rate decreases in proportion to the decreasing pressure difference between the reservoir and the processing facility. At low oil flow rates, a well becomes unstable and this leads to reduced production and processing problems. The formation of slug flow in pipelines, particularly at bends in the vertical plane is a manifestation of such instability.

The description and classification multi-phase flows in a pipe or tube (figure 1), and the use of flow-maps (figure 2) to estimate expected flow regimes under given circumstances is well-established (Butterworth & Hewitt 1977).

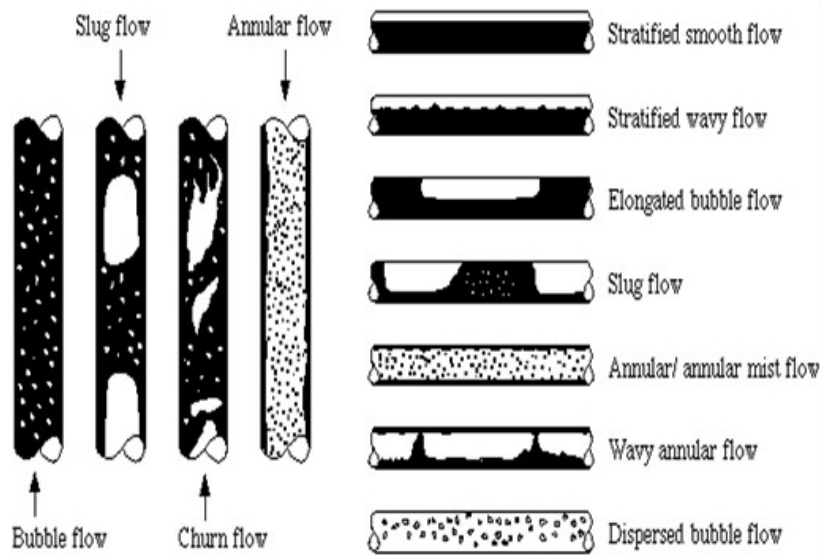


Figure 1: Two-phase flow regimes

The incidence of different flow patterns depends on the relative flow rates of each component. The characteristics of slug flow are intermittency and gas entrainment at the front of the propagating slug. In this case multi-phase fluid slugs may travel at velocities of up to  $2 - 3 \text{ ms}^{-1}$  along the inside of a pipe, each filling the full cross-section over a finite length and each bounded before and after by stratified flows. There is a strong dependence on initial conditions, and on pipe inclination, as shown in figure 3. In this context, the total flow comprises a mixture of oil, water, gas and solid particles; it is almost always fully turbulent with complex free boundaries and subject to multi-scale effects. The presence of slug flow at a given point along a pipeline may be manifested by apparently random variations, with respect to time, of pressure (188 – 196 bar), gas

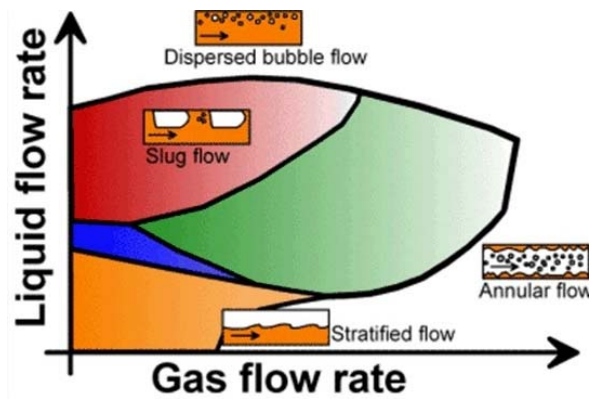


Figure 2: Two-phase flow map

volume flow rate ( $1 - 20 \text{ Sm}^3 \text{ hr}^{-1}$ ), and oil volume flow rate ( $0 - 80 \text{ Sm}^3 \text{ hr}^{-1}$ )<sup>1</sup>, where the exemplified numerical ranges are from figure 3. Large slugs are difficult to handle and potentially damaging for processing units.

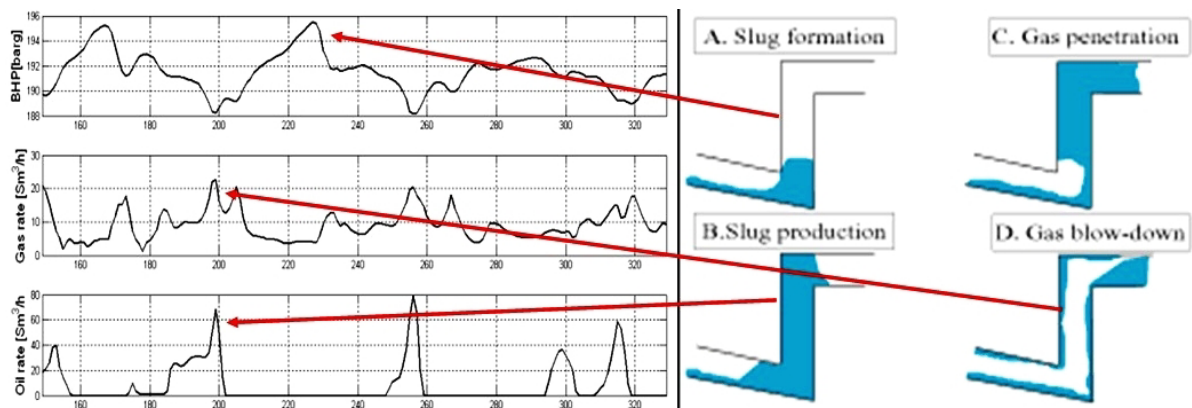


Figure 3: Transients for a bend in the vertical plane

The front of a slug may be regarded as a propagating, continuously breaking wave, which continuously entrains gas. The amount of gas entrainment has a large impact on flow pattern, pressure drop, and the slug length and propagation velocity, each of which affect decisions about how to optimise production. Hence the interest of Hydro in gaining better understanding of gas entrainment in the slug flow regime. In particular, the Study Group was asked to

- explore alternative or new ways to treat the entrainment problem;
- improve understanding of physical processes governing entrainment;
- suggest models for the various phenomena.

<sup>1</sup> $\text{Sm}^3$  is the unit of *standard volume* at  $15^\circ\text{C}$  and  $1.013 \text{ bar}$  (one standard atmosphere). In the case of oil, it is the volume after dissolved and entrained gases have been removed.

## 1.2 Current understanding and challenges

### 1.2.1 Theory and modelling

Understanding the physics of the gas-entrainment process at the slug front is difficult, because of the complex turbulence phenomena, a large fraction of bubbles influencing the turbulent properties, bubble-bubble interactions (coalescence and break-up), and other effects. It is beyond current modelling capabilities to describe the slug flow process from first principles. There are a number of simplified models of entrainment in slug flow, but few capture any essential physics of the entrainment process. There is little consensus regarding the physical effects that govern entrainment rate or what the precise influence is of physical properties (densities, viscosities, surface tension, etc) on the entrainment rate. There are six dimensionless groups which may be important in modelling gas entrainment.

### 1.2.2 Experiments and data

Current understanding is based upon data from a number of experiments, but none covers the full space of variables; moreover, there is a lack of experimental data at high pressures, where buoyancy forces are strongly reduced.

Experiments with density measurements provide a relation between the mean volume fraction of gas in the slug as a function of the liquid and gas volume fluxes,  $Q_l$  and  $Q_g$ , but such ‘correlations’ are system specific and provide little data on the mechanisms of entrainment.

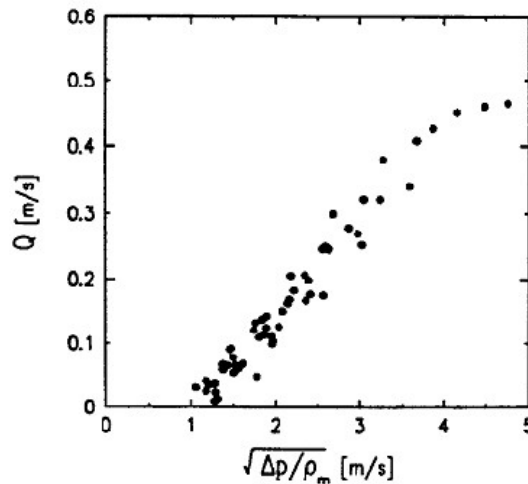


Figure 4: Slug entrainment rate for a ‘push-in’ experiment, from Nydal & Andreussi (1991).

In ‘push in’ experiments, a liquid plug is pushed into a pipe containing a liquid layer. Such experiments indicate that the entrainment rate is proportional to pressure drop

at the slug front (see figure 4, but it is likely that such result are dependent on fluid properties and pipe dimensions. During the week, Study Group participants visited Barry Azzopardi's slug flow experimental facility at Nottingham University. (See figure 5.)



Figure 5: Barry Azzopardi's slug flow experimental facility at Nottingham University. A slug is travelling from right to left in the picture.

The unsteady nature of slug flow, means that it is a major challenge to obtain good and accurate measured data for gas entrainment at the slug front. To overcome this problem, experiments have been performed (Julshamn 2006) in which a steady hydraulic jump is created in a pipe, enabling direct measurement of gas entrainment rates for different pipe diameters and fluid properties (density, viscosity and surface tension). See, for example, the arrangement in figure 6. Such experiments indicate that, in stationary hydraulic jumps, entrainment is proportional to the Froude number of the upstream liquid film, although there are no data on the influence of gas density. See figure 7.

### 1.3 Data provided to the Study Group

Hydro provided to the Study Group a copy of Julshamn's PhD thesis (Julshamn 2006). Julshamn's thesis is about stationary hydraulic jumps, as depicted in figure 6. It contains measurements of the air flow rate necessary to establish a stationary hydraulic jump for a given liquid flow rate. See figure 7.

The thesis also has measurements of the pressure difference across the hydraulic jump, and of the bubble size distributions downstream of the jump. It has many still pictures, and formulates a model somewhat like that reported in section 4 below, though with various extra approximations.

In Julshamn's observation that more viscous flows entrain less (or at least look less foamy), there is some support for the argument, at the end of section 4 of this report,

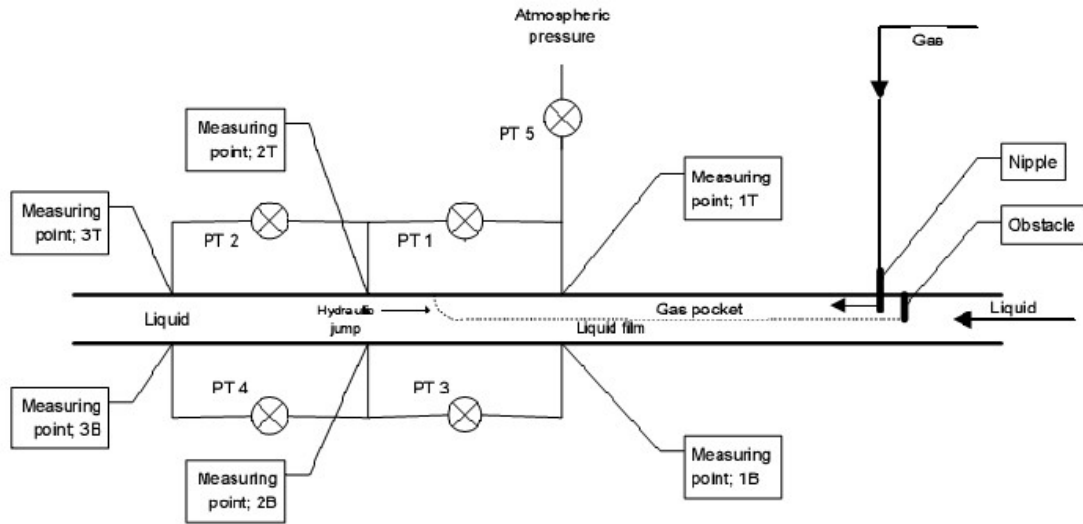


Figure 6: Experimental arrangement for a stationary hydraulic jump, from Julshamn (2006).

for entrainment being proportional to turbulence levels. However, it is not clear whether the velocities were the same for the different fluids.

## 2 Literature survey and approaches adopted

A literature survey revealed a vast number of publications on two-phase flow over many decades and many in the area of slug flow, much of it addressing correlations for the slug flow regime. Aside from Julshamn's work (2006), there are models for hydraulic jumps or bores, which have a single shock boundary (see for example Ockendon & Ockendon (2004)). However, as basis for approaching the slug flow gas entrainment problem in the Study Group, attention was given to modelling the propagation of slugs (which have two shock boundaries).

Also found was work (particularly observational and experimental) on air entrainment in hydraulic jumps and breaking waves, but less on the relationship between air entrainment and energy loss, some of which is briefly reviewed below.

### 2.1 Energy dissipation and air entrainment

Experimental work on air entrainment in plunging breakers is exemplified by Chanson *et al.* (2002) for which the entrainment is via the mechanism of the top of the wave forming a water jet which runs ahead of the wave face and entraining air when it impacts the free water surface ahead of the wave. This work provides evidence of the rise in free surface level caused by entrainment for void fractions up to a maximum of  $\sim 12\%$  in the

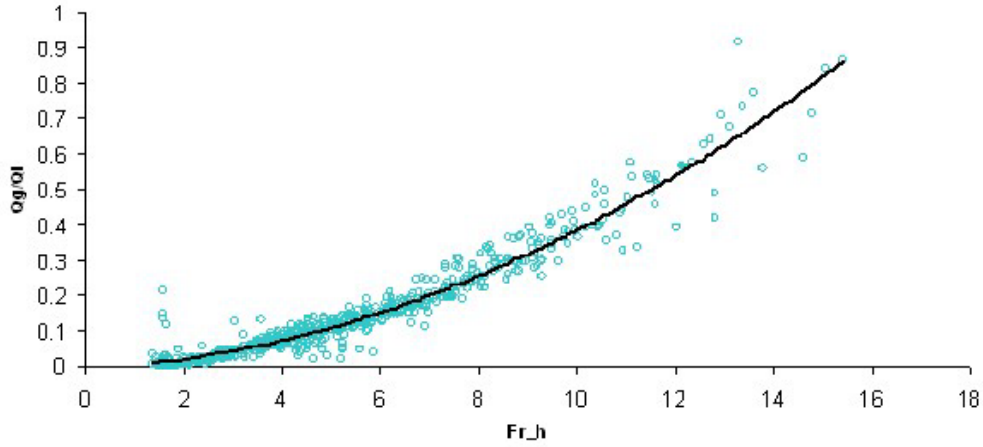


Figure 7: Entrainment rate as function of upstream Froude number for a stationary hydraulic jump, from Julshamn (2006).

jet impact zone, and also suggests that bubble rise velocity is nearly constant for bubble diameters ranging from 0.5 – 50 mm. The effect on the wave field of bulking (increase in volume) caused by entrainment is also investigated.

An attempt at modelling the energy dissipation due to bubble entrainment is made by Hoque & Aoki (2005), and it includes an analysis of a hydraulic jump. Using measured void fraction data and a simple model based on the ongoing work done in raising the centre of gravity of fluid at the jump front through bubble entrainment, Hoque & Aoki suggest that  $\sim 25\%$  of the total hydraulic jump energy loss  $E_H$  is dissipated in this way. Here

$$E_H = \rho_l g V_1 d_1 \frac{(d_2 - d_1)^3}{4d_1 d_2}, \quad (1)$$

where the depth  $d$  and velocity  $V$  at the inlet and outlet are indicated by subscripts 1 and 2 respectively, and  $d_2 > d_1$ . Hoque & Aoki report that their fraction of  $\sim 25\%$  energy dissipation through bubble entrainment is consistent with the values of 30 – 50% reported in work by Lamarre & Melville (1991) on breaking waves. Very much smaller (1 – 2%) bubble entrainment dissipation ratios were calculated by Hoque & Aoki (2005) for vertical plunging jets.

### 3 Travelling slugs

The following models of travelling slug flow are expressed in terms of the variables and parameters depicted in figure 8.  $U$  denotes the slug velocity and  $u$  a flow velocity.  $\rho$  denotes density, and (when not a suffix)  $g$  the gravitational constant. The internal height of the pipe is  $H$ , and  $h$  denotes the height of the liquid–gas boundary of the stratified flow.  $P$  and  $p$  denote pressure. Subscripts  $L$  and  $R$  denote the left (trailing) and right (leading) edges of a slug, and the subscripts  $l$  and  $g$  respectively denote a property of the liquid and gas states.

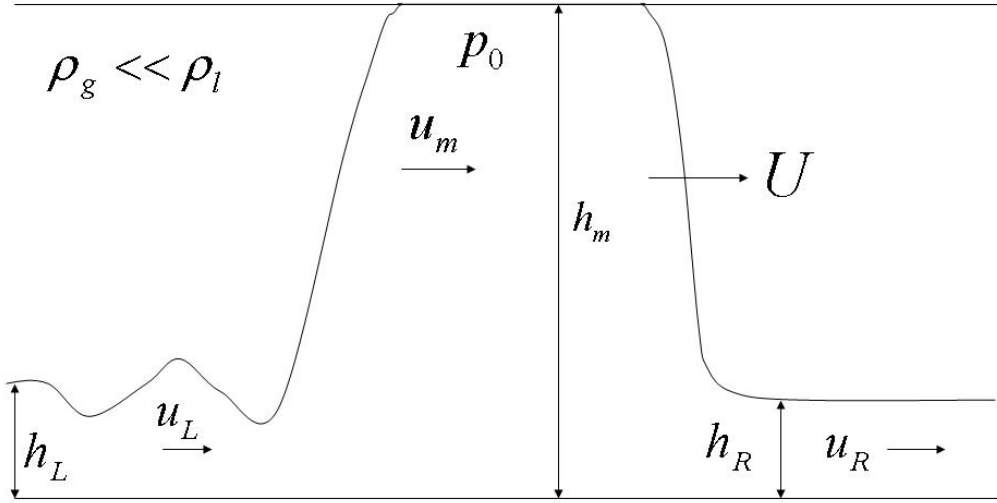


Figure 8: Horizontal pipe: variables and parameters for the travelling slug

### 3.1 Horizontal pipe

We assume a one dimensional shallow water model for a homogeneous fluid, and write down equations for the conservation of mass, momentum, and energy:

$$\partial_t h + \partial_x(hu) = 0, \quad (2)$$

$$\partial_t(hu) + \partial_x\left(hu^2 + \frac{1}{2}gh^2\right) = 0, \quad (3)$$

$$\partial_t\left(\frac{1}{2}hu^2 + \frac{1}{2}gh^2\right) + \partial_x\left(\frac{1}{2}hu^3 + \frac{1}{2}gh^2u\right) = 0. \quad (4)$$

The integrated forms of these three conservation equations provide three jump conditions, but there are only two variables  $h$  and  $u$ . We now assume that

- the leading shock front conserves mass and momentum, but dissipates energy;
- the trailing undular bore conserves mass and energy, but radiates momentum,

as depicted in figures 8 and 9.

Previous work (Fan *et al.* 1993) has considered a hydraulic jump at the front, and a so-called Benjamin (1968) bubble at the back. Observations made of the experiment

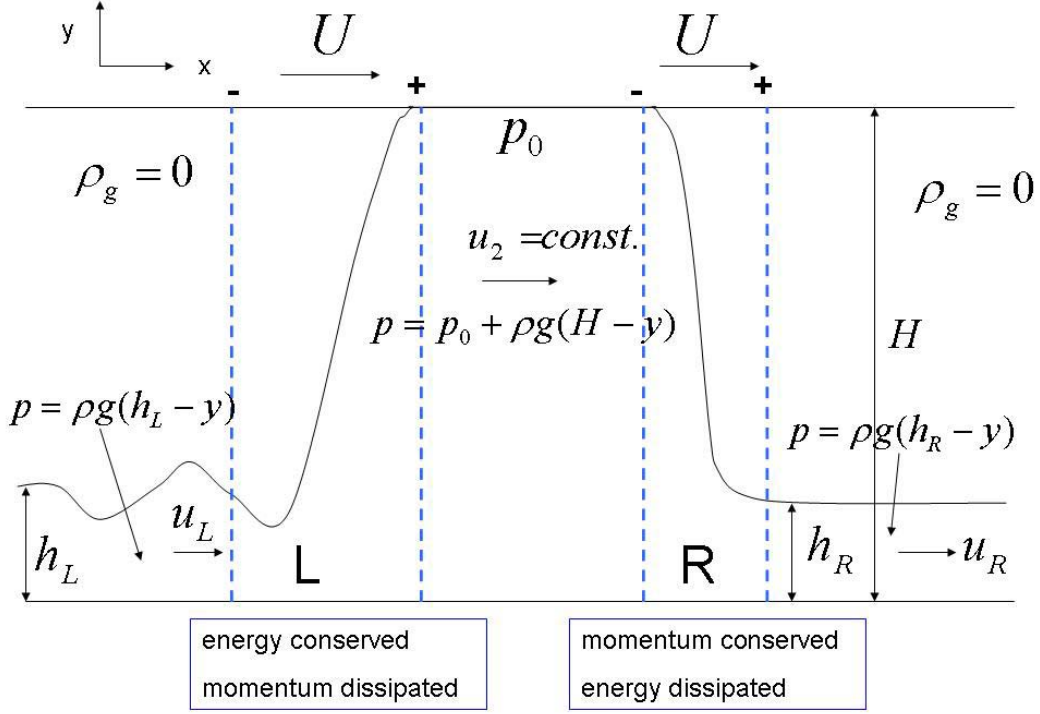


Figure 9: Horizontal pipe: scheme for mass, energy and momentum balances

depicted in figure 5, seemed to support the assumption that  $h_L = h_R = h$ , and that both shocks move at the same speed  $u$ . Let  $\delta = h/H$ .

The equations for **conservation of mass** at the left (L) and right (R) shock planes (as depicted in figure 9) are

$$\begin{aligned} L : [h(u - U)]_{\pm}^{\pm} &= 0 \\ R : [h(U - u)]_{\pm}^{\pm} &= 0, \end{aligned} \quad (5)$$

which imply that

$$\begin{aligned} u_L &= u_R = u_1 \\ u_2 - U &= \delta(u_1 - U). \end{aligned} \quad (6)$$

The **conservation of momentum** at R gives

$$[\rho h(u - U)^2 + \frac{1}{2}\rho g h^2]_{\pm}^{\pm} - \rho_0 H = 0, \quad (7)$$

while the **conservation of energy** at L gives

$$\frac{\rho}{2g}[(U^2 + gh)(U - u)]_{\pm}^{\pm} - \frac{\rho g}{2}[h^2 u]_{\pm}^{\pm} - P_0 U_2 H = 0. \quad (8)$$

It was not at first apparent that this model has a serious deficiency. The assumptions  $h_L = h_R$  and  $U_L = U_R$ , if taken at face value, assert that the shallow water expressions for the energy and momentum downstream of the slug are equal to the expressions for the energy and momentum upstream respectively. The model, however, assumes that energy is dissipated at the leading hydraulic jump (at  $R$ ), and that momentum is dissipated at the trailing undular bore (at  $L$ ). Solving the correct Rankine–Hugoniot jump conditions then leads to the conclusion that the jump (at  $R$ ) and the bore (at  $L$ ) are two infinitesimally weak (and thus reversible) shocks propagating with the fluid speed. The slug speed  $U$  thus equals both  $U_L$  and  $U_R$ .

In hindsight, the energy required to entrain bubbles at the leading hydraulic jump is found to be very small compared with the energy available in the oncoming flow. (See Section 4.) Thus, one could easily gain the impression by eye, watching slugs in an experimental set up like the one shown in figure 5, that the upstream and downstream flow parameters ( $h$  and  $U$ ) are precisely equal, rather than just very close to each other.

In addition, the momentum lost from one member of a train of slugs through waves radiating from a trailing undular bore would enter the leading hydraulic jump of the next slug behind in the train.

### 3.2 Inclined pipe for $Fr \gg 1$

We now proceed with the analysis of the inclined pipe for large Froude number ( $Fr \gg 1$ ), without assuming that  $h_L = h_R = h$ . See figure 10.

The equations for **conservation of mass** at R and at L are

$$R : (u_1^+ - U)h_1^+ = (u_2 - U)H \quad (9a)$$

$$L : (u_1^- - U)h_1^- = (u_2 - U)H. \quad (9b)$$

The **conservation of momentum** at the leading edge R of the slug is

$$(u_1^+ - U)^2 h_1^+ = (u_1 - U)^2 H - (P - p_\infty^+)H, \quad (10)$$

and the **conservation of energy** at the trailing edge L of the slug is

$$\frac{1}{2}(u_1^-)^2(u_1^- - U) - \frac{1}{2}(u_2)^2(u_2 - U) = (p_\infty^- - P)u_2 H. \quad (11)$$

The pressure drop in the slug is

$$p_\infty^+ - p_\infty^- = -gL_s \sin(\alpha), \quad (12)$$

and the pressure drop in the film is

$$\frac{1}{2}(U - u_1^+)^2 - \frac{1}{2}(U - u_1^-)^2 = gL_g \sin(\alpha). \quad (13)$$

We prescribe the liquid flux

$$Q_t = u_1^+ h_1^+, \quad (14)$$

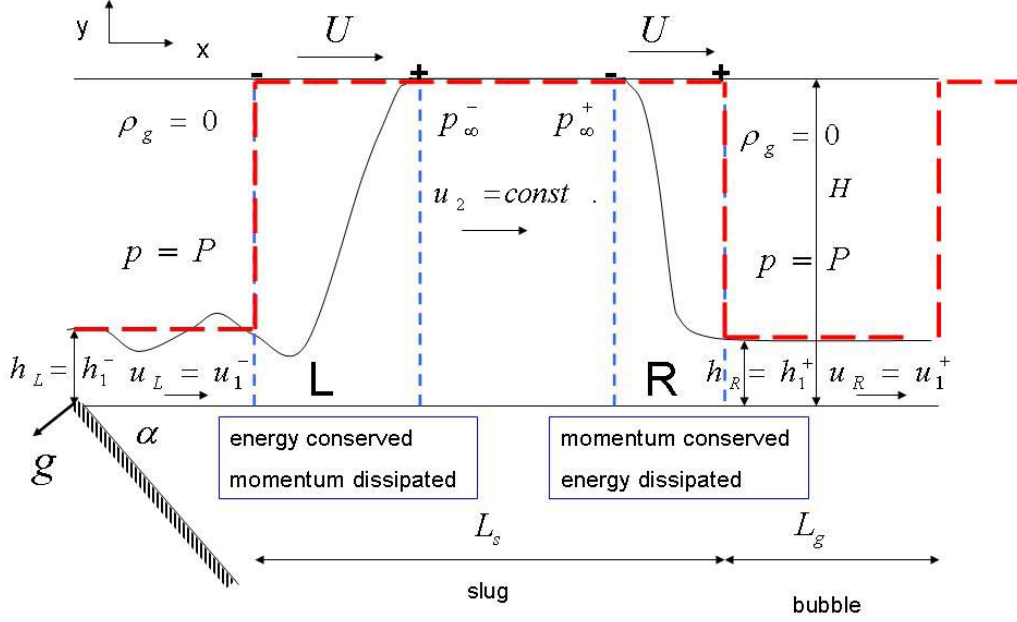


Figure 10: Inclined pipe: scheme for mass, energy and momentum balances

and the gas flux

$$Q_g \approx UH \frac{L_g}{L_g + L_s}. \quad (15)$$

Without loss of generality, we can take  $P = 0$ .

Thus, we have 8 equations and 10 unknowns, which therefore have a two parameter family of solutions. What selection criteria can be used? Further work is required; for example, taking the pressure drop in equations (12) and (13) to be purely hydrostatic seems inconsistent with assuming large Froude number and hence weak gravity.

### 3.3 Inviscid 2D potential flow

Lee & Vanden-Broeck (1999) have carried out an analysis of the flow of two-dimensional bubbles in an inclined tube of inviscid fluid. As the inclination angle  $\alpha$  of the tube from the horizontal increases, they find that the critical Froude number  $Fr^*(\alpha)$ , below which a slug bubble may exist, increases from 0.4 to above 0.5 and then decreases to 0.3 in the vertical position. (Here, we are concerned with  $0 \leq \alpha \leq \pi/2$ .) This result is in good agreement with Bendikson's (1984) experimental measurements of  $Fr^*(\alpha)$ . Lee & Vanden-Broeck (1999) also gave the velocity of a bubble in moving fluid as

$$U = C_B U_{\text{liquid}} + U_0, \quad (16)$$

but with  $C_B = 1$  instead of Bendikson's value  $C_B = 1.2$ . Here  $U_0$  is the speed of a bubble in quiescent liquid, and  $U_{\text{liquid}}$  is the speed of any additional motion of the liquid relative to the tube walls.

However, Lee & Vanden-Broeck's (1999) theory is for inviscid fluids, and therefore invariant under Galilean transformations along the axis of the tube. This explains why  $C_B = 1$  precisely in their theory. A bubble in a real fluid will experience viscous drag when moving relative to the tube walls. The tube therefore defines a preferred frame, which is why the experimental value of  $C_B$  differs from the inviscid value.

## 4 Entrainment - energy dissipation rate

We now provide an approximate analysis of the gas entrainment in the leading edge of the slug in the horizontal pipe configuration. The domain of analysis is depicted in figure 11. We assume a homogeneous mixture of gas and liquid with a void fraction  $\phi$ , and a single velocity  $U_m$ . We thus neglect any relative motion between the bubbles and the liquid.

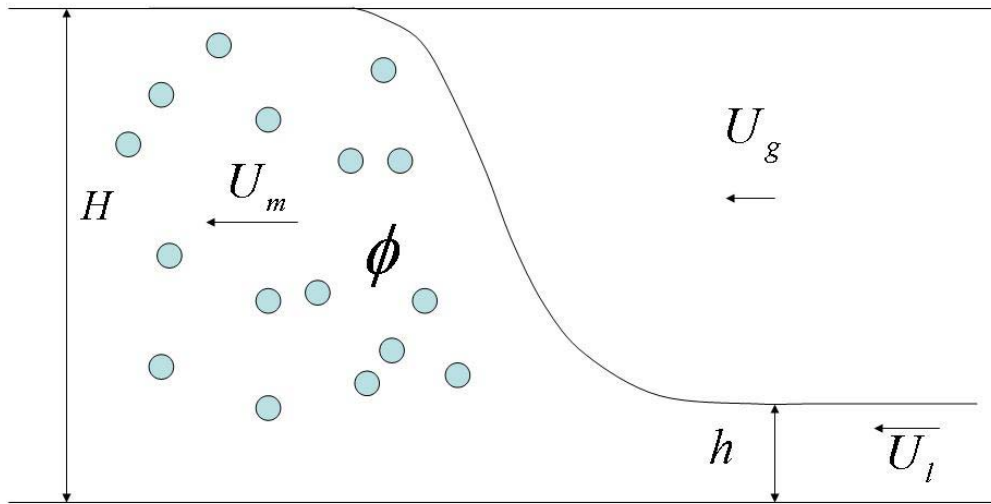


Figure 11: Scheme for modelling gas entrainment rate

The experimentally-measured pressure jump is of the order of 1 kPa, the same order of magnitude as the hydrostatic pressure difference across a few centimetres of water.

These two pressures are both much smaller than atmospheric pressure,  $1 \text{ atm} \sim 10^5 \text{ Pa}$ , so we ignore any compression of the gas phase due to changes in pressure.

Conservation of mass (now equivalent to conservation of volume) for the liquid and gas phases then gives

$$HU_m\phi = (H - h)U_g \quad (17a)$$

$$HU_m(1 - \phi) = hU_l \quad (17b)$$

for a steady hydraulic jump. Solving for the void fraction  $\phi$ , we obtain

$$\phi = \frac{1}{1 + \frac{hU_l}{(H - h)U_g}}. \quad (18)$$

The **momentum conservation** determines the pressure jump, and the **energy equation** determines the dissipation rate. We are thus left without any relation between the three upstream quantities  $h$ ,  $U_l$ ,  $U_g$  of the kind that might explain figure 7.

How much energy is required to create bubbles? The void fraction  $\phi$  may be rewritten as

$$\phi = \frac{4}{3}\pi r^3 n, \quad (19)$$

in terms of a typical bubble radius  $r$ , and the number of bubbles  $n$  per unit volume. The surface energy per unit volume is then

$$E_s = 4\pi r^2 \gamma n = 3\phi \gamma / r, \quad (20)$$

where  $\gamma$  is the surface tension of an air/liquid interface.

The engineering literature (*e.g.* Barnea *et al.* 1982, Brauner & Ullmann 2004) assumes that the bubble radius  $r$  should be estimated by the critical radius  $r_c$  for which surface tension, tending to create spherical bubbles, just balances the distorting effects of buoyancy,

$$r_c = \left( \frac{0.4\gamma}{(\rho_l - \rho_g)g} \right)^{1/2} \sim 1 \text{ mm}, \quad (21)$$

when evaluated using  $\gamma \sim 3 \times 10^{-2} \text{ Nm}^{-1}$  for a kerosene and air mixture.

The surface energy per unit volume is then

$$E_s \sim 100\phi \text{ Nm}^{-2} \sim 0.1\phi \text{ kPa}, \quad (22)$$

which is much smaller than the pressure drop across the hydraulic jump (typically 1 kPa as above). At first sight, it therefore seems unlikely that the surface energy of bubbles is responsible for setting the void fraction downstream of the hydraulic jump. A hypothesis relating surface energy to energy dissipation was considered early in the week, but discarded on the basis of these order-of-magnitude estimates.

However, a similar hypothesis *is* used in the engineering literature (Chen *et al.* 1997, Zhang *et al.* 2003), but with the modification that only the *turbulent* part of the kinetic energy of the upstream flow is available for creating bubbles. The Reynolds number based on the upstream flow is large, so the flow will typically be turbulent. There will thus be many small-scale turbulent fluctuations superimposed upon the mean flow, the flow indicated by the velocity  $U_l$  in figure 11. The fluctuations are usually defined as deviations from some spatially-averaged flow field.

The magnitude of the fluctuations is typically estimated using the friction velocity  $u^*$ ,

$$u^* = (\tau/\rho_L)^{1/2}, \quad (23)$$

where  $\tau$  is the shear stress at the wall, and  $\rho_L$  the density of the liquid phase. The mean streamwise velocity  $U_l$  is related to the friction velocity  $u^*$  via the log-law velocity profile equation

$$\frac{U_l}{u^*} = \frac{1}{k} \log Re^* + 5.5, \quad \text{where } Re^* = \frac{H u^*}{\nu} = Re \frac{u^*}{U_l}. \quad (24)$$

$Re^*$  is the Reynolds number based on the friction velocity  $u^*$ ,  $k = 0.4$  is von Karman's constant, and 5.5 is another empirical constant. Equation (24) is often rewritten in terms of the Fanning friction factor  $f_F = 2u^{*2}/U_l^2$ ,

$$f_F^{-1/2} = 4 \log_{10}(Re f_F^{1/2}) - 0.4, \quad (25)$$

as in equation (19) of Goldstein (1938), §154, though using  $\gamma$  instead of  $f_F$ . Thus  $\frac{1}{2}f_F = u^{*2}/U_l^2$  is the fraction of the kinetic energy associated with turbulent eddies.

For  $Re \lesssim 10^5$ , Blasius proposed an approximate explicit formula for  $f_F$ , equation 20 in Goldstein (1938) §155,

$$f_F = 0.0665(U_l H/\nu)^{-1/4} = 0.0665 Re^{-1/4}. \quad (26)$$

Julshamm's experiments were characterised by friction factors in the range  $0.015 \leq f_F \leq 0.035$ , corresponding to Reynolds numbers in the range  $7000 \leq Re \leq 160\,000$ . Balancing the surface energy given by (22) with the friction factor that multiplies the pressure drop (typically 1 kPa) across the hydraulic jump, we get

$$0.1\phi \sim f_F, \quad \text{so} \quad 0.15 \leq \phi \leq 0.35,$$

which is not unreasonable.

Andritsos & Hanratty (1987) have suggested that waves on the gas/liquid interface may lead to a larger effective friction factor, which leads into the following section on long wave models for the onset of a hydraulic jump.

## 5 Long wave model

This approach is based on the idea of a simple dynamical model to determine the pressure conditions for the onset of slug flow. The configuration for the analysis is depicted in figure 12.

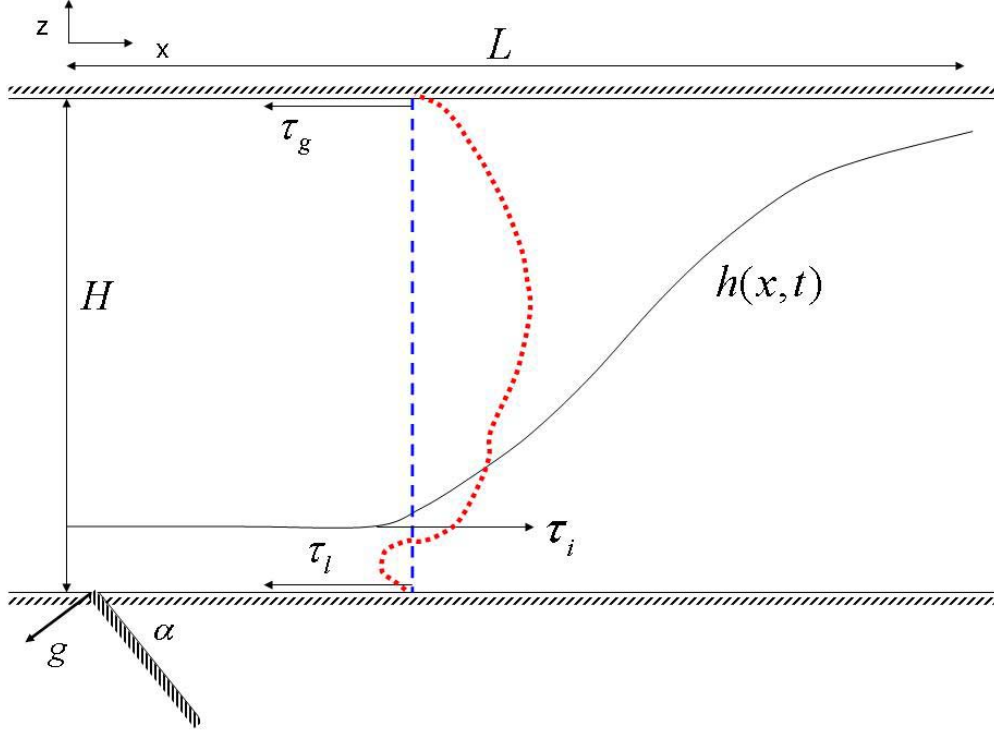


Figure 12: Scheme for the long wave model

Assume the pressure is solved by

$$\frac{\partial}{\partial x} \int_0^1 u dz = 0, \quad (27)$$

with  $u$  taking different values in the liquid phase ( $z < h$ ) and the gas phase ( $z > h$ ).

Conservation of the masses of liquid and gas then gives the following relations

$$h_t + \frac{\partial}{\partial x} \int_0^h u dz = -J \quad (28a)$$

$$\phi + \frac{\phi_x}{h} \int_0^h u dz = -J, \quad (28b)$$

where  $J$  is the mass flux of gas into the liquid. If we assume that  $J = -\mu_e h_{xx}$ , then entrainment would act to stabilize the interface, which suggests that a better model for  $J$  should be investigated.

The main point would be to find an entrainment model  $J$  which is based on the local vorticity of the flow, and which depends on void fraction. Any velocity difference between the liquid and gas velocities tends to cause Kelvin–Helmholtz instabilities at the liquid/gas interface. Conversely, the larger density of the liquid will tend to stabilise disturbances of the interface, but entrainment of gas will reduce the density of the lower,

predominantly liquid, phase. The rolling up of Kelvin–Helmholtz billows formed through these two competing mechanisms is a natural model for entrainment. A model for  $J$  can then be put into equations (28) to close the model.

Could entrainment be the mechanism that, when included, resolved the following issues? That is, to the left of L in figure 10, entrainment provides the momentum ‘dissipation’, while at R bubbles under the slug moving into the gas ‘dissipate’ energy? Is it possible to put in a fixed mass flux  $J$  and see if the momentum/energy jumps that are consistent with this mass flux are also consistent with dissipation for each of these layers?

## 6 Conclusions

The work reported must be regarded as in progress. Although the objective is to better understand gas entrainment in slug flow, much of the effort during the Study Group was expended on developing models of the phenomenon of slug flow and its onset, as a foundation for studying the gas entrainment processes. The following areas are suggested for further work.

- A feature of the derived model of slug flow for large Froude number is that the number of equations is two less than the number of unknowns. Thus, for example the length of the slug is undetermined. The model is based on momentum loss at one end of the slug and energy loss at the other, and an assumed purely hydrostatic pressure drop across the slug in the inclined pipe case. Further study of this model is required.
- During the Study Group the notion of undular bores emitting waves from one slug that feed momentum into the next slug along was discussed. Subsequently, there has emerged the idea of developing a long wave model (something like shallow water with a lid) that would support waves propagating from slug to slug, to study the dynamics of trains of slugs.
- The work on gas entrainment focused on the hydraulic jump and found the surface energy per unit volume of bubbles to be between 1 and 2 orders of magnitude lower than the pressure drop across the jump. This is substantially less than the 25% suggested in Hoque & Aoki (2005) for entrainment energy loss in hydraulic jumps, but closer to the 1 – 2% reported by them for vertical plunging jets. Having originally rejected a link between kinetic energy dissipation and formation of bubble surface energies, based on order-of-magnitude estimates, the Study Group later began investigating the suggestion in the literature that only the turbulent part of the upstream flow is available for the creation of bubbles. In pursuit of this suggestion, preliminary work on friction factors reported here finds that the turbulent energy is consistent with bubble surface energies for void fractions in the range  $0.15 \leq \phi \leq 0.35$ . Further work is required to properly study this encouraging finding.

- The Study Group gave attention primarily to the large Froude number approximation, as in Julshamn's thesis (Julshamn 2006), which neglects hydrostatic pressures. The finite Froude number analysis is believed to be tractable and is worthy of further work.
- Work was also started on a long wave model to gain insight into the conditions for the onset of slug flow and a mechanism whereby entrainment acts to stabilise leading the surface of the slug or jump. Further work is required to develop and investigate a void fraction dependent entrainment model based on local flow vorticity.

## References

- ANDRITSOS, N. & HANRATTY, J. T. (1987) Influence of interfacial waves in stratified gas-liquid flows. *AIChE J.* **33**, 444–454.
- BARNEA, D., SHOHAM, O. & TAITEL, Y. (1982) Flow pattern transition for vertical downward two phase flow. *Chem. Eng. Sci.* **37**, 741–744.
- BENDIKSEN, K. H. (1984) An experimental investigation of the motion of long bubbles in inclined tubes. *Int. J. Multiphase Flow* **10**, 467–483.
- BENJAMIN, T. (1968) Gravity currents and related phenomena. *J. Fluid Mech.* **31**, 209–248.
- BRAUNER, N. & ULLMANN, A. (2004) Modelling of gas entrainment from Taylor bubbles. Part B: A stationary bubble. *Int. J. Multiphase Flow* **30**, 273–290.
- BUTTERWORTH, D. & HEWITT, G. F. (1977) *Two-Phase Flow and Heat Transfer*. Oxford: Oxford University Press.
- CHANSON, H., AOKI, S.-I. & MARUYAMA, M. (2002) Unsteady air bubble entrainment and detrainment at a plunging breaker: dominant time scales and similarity of water level variations. *Coastal Eng.* **46**, 139–157.
- CHEN, X. T., CAI, X. D. & BRILL, J. P. (1997) A general model for transition to dispersed bubble flow. *Chem. Eng. Sci.* **52**, 4373–4380.
- FAN, Z., RUDER, Z. & HANRATTY, T. J. (1993) Pressure profiles for slugs in horizontal pipelines. *Int. J. Multiphase Flow* **19**, 421–437.
- GOLDSTEIN, S., ed. (1938) *Modern Developments in Fluid Dynamics*. Oxford: Oxford University Press.
- HOQUE, A. & AOKI, S.-I. (2005) A quantitative analysis of energy dissipation among three typical air entrainment phenomena. *Environ. Fluid Mech.* **5**, 325–340.
- JULSHAMN, J. A. (2006) Hydraulic jumps in horizontal two-phase pipe flow. PhD thesis, Norwegian University of Science and Technology (NTNU), Trondheim.

- LAMARRE, E. & MELVILLE, W. K. (1991) Air entrainment and dissipation in breaking waves. *Nature* **351**, 469–472.
- LEE, J. & VANDEN-BROECK, J.-M. (1999) Bubbles rising in an inclined two-dimensional tube and jets falling along a wall. *J. Austral. Math. Soc. Ser. B* **39**, 332–349.
- NYDAL, O. J. & ANDREUSSI, P. (1991) Gas entrainment in a long liquid slug advancing in a near horizontal pipe. *Int. J. Multiphase Flow* **17**, 179–189.
- OCKENDON, H. & OCKENDON, J. R. (2004) *Waves and Compressible Flow*. Springer.
- ZHANG, H.-Q., WANG, Q., SARICA, C. & BRILL, J. P. (2003) A unified mechanistic model for slug liquid holdup and transition between slug and dispersed bubble flows. *Int. J. Multiphase Flow* **29**, 97–107.